Microrheology Probes Length Scale Dependent Rheology

J. Liu,[1] M. L. Gardel,[1,*] K. Kroy,[2] E. Frey,[3] B. D. Hoffman,[4] J. C. Crocker,[4] A. R. Bausch,[5] and D. A. Weitz[1]

[1]*Dept. of Physics & DEAS, Harvard University, Cambridge, Massachusetts 02138, USA*
[2]*ITP, Universität Leipzig, D-04103 Leipzig, Germany*
[3]*Ludwig-Maximilians-Universität, München, Germany*
[4]*Dept. of Chemical Engineering, University of Pennsylvania, Philadelphia, Pennsylvania 19104, USA*
[5]*Physik-Dept E22, Technische Universität München, D-85748 Garching, Germany*

(Received 1 October 2005; published 23 March 2006)

We exploit the power of microrheology to measure the viscoelasticity of entangled F-actin solutions at different length scales from 1 to 100 μm over a wide frequency range. We compare the behavior of single probe-particle motion to that of the correlated motion of two particles. By varying the average length of the filaments, we identify fluctuations that dissipate diffusively over the filament length. These provide an important relaxation mechanism of the elasticity between 0.1 and 30 rad/sec.

DOI: 10.1103/PhysRevLett.96.118104 PACS numbers: 87.15.La, 83.10.Mj, 83.80.Lz, 87.16.Ka

Semiflexible polymer solutions exhibit a rich mechanical behavior which is due to contributions from structure and relaxation dynamics at many different length scales [1–5]. Single filaments are characterized by their average contour length, L, and by their persistence length, $l_p = \kappa/k_BT$, where k_BT is the thermal energy and κ is their bending rigidity. Because of their large l_p, semiflexible polymers become entangled at very low concentrations with an elastic modulus enhanced by comparison to flexible polymers at similar concentrations. Such solutions are characterized by the average distance between polymers, or mesh size, ξ. However, filaments are sterically hindered at the entanglement length, $l_e \sim \xi^{4/5} l_p^{1/5}$, instead of ξ, as is the case for flexible polymers [3,6]. An excellent model for semiflexible polymers is the cytoskeletal protein, filamentous actin (F-actin), which has $l_p \sim 15$ μm [7,8], much larger than its diameter, $d \sim 7$ nm [9]. The mesh size of entangled F-actin solutions is given by $\xi = 0.3/\sqrt{c_A}$, where c_A is the actin concentration in mg/mL and ξ is in microns [10]. In addition, L can be regulated through addition of the actin severing and capping protein, gelsolin [11]. In entangled F-actin solutions, the elastic modulus $G'(\omega)$ and the loss modulus $G''(\omega)$ are dominated by single-filament dynamics at frequencies $\omega >$ 100 rad/sec, and exhibit a scaling of $\omega^{3/4}$ [1]. The lowest frequency of this regime is determined by the relaxation time of bending fluctuations over an entanglement length, $\tau_e \approx \varsigma l_e^4/l_p k_B T$, where ς is the effective friction coefficient of the filament in solution [12]. For $\omega < \tau_e^{-1}$, steric hindrance leads to a frequency-independent elastic plateau modulus, $G_0 \sim k_BT/\xi^2 l_e$ over a wide frequency range [12]. Neither of these regimes should depend on L. However, at intermediate frequencies, bulk rheology experiments reveal a transition regime where the mechanical response is highly dependent on L [13]. These results cannot be explained by single-filament models that do describe both the high and low frequency viscoelasticity. Surprisingly, there have been no attempts to identify the relaxation mechanisms in this transition regime.

In this Letter, we exploit microrheology to directly probe the mechanical response of entangled F-actin solutions at length scales from 1 to 100 μm as we vary both mesh size and average filament length. We identify fluctuations that dissipate diffusively over L as an important relaxation mechanism for elasticity between 0.1 and 30 rad/sec. Two-particle (2P) microrheology is used to probe fluctuations at large lengths (>5 μm), giving a good approximation of bulk rheology [14], whereas one-particle (1P) microrheology is used to isolate contributions of short-length fluctuations ($\sim l_e$) [15]. For a given mesh size, 1P microrheology exhibits a rapid transition from the single-filament regime to the plateau regime. The transition is independent of L, but is sensitive to l_e. However, 2P microrheology shows enhanced viscoelastic relaxation at intermediate frequencies. The relaxation time of these additional fluctuations scales as L^2, consistent with diffusion over the filament length up to l_p [12]. Thus, we characterize length-scale-dependent rheology and identify an important contribution to the mechanical response.

Monomeric-actin (G-actin) solutions are prepared by dissolving lyophilized G-actin in Millipore water and dialyzing against G-buffer (2 mM Tris HCl, 0.2 mM ATP, 0.2 mM $CaCl_2$, 0.2 mM DTT, 0.005% NaN_3, pH 8.0) at 4 °C for 24 hours; the solutions are used within seven days. G-actin is mixed with polystyrene particles of radius $a =$ 0.42 μm, coated with methoxy-terminated poly(ethylene glycol) to prevent nonspecific binding of protein to the bead surface [16]. Modifying the surface chemistry of the particles has only a small effect on the particle mobility [16]; this suggests that local heterogeneities, such as those due to depletion or binding to the bead, have little influence on these microrheology measurements. We vary L through the addition of gelsolin [11]. Actin polymerization is initiated by adding 1/10 of the final volume of 10x F-buffer

(20 mM Tris HCl, 20 mM $MgCl_2$, 1 M KCl, 2 mM DTT, 2 mM $CaCl_2$, 5 mM ATP, pH 7.5) and mixing gently for 10 seconds. The sample is loaded into a glass chamber and sealed with high-vacuum grease. After equilibrating for 1 h at room temperature, the sample is imaged with an inverted microscope in bright field (objective: 63x; N.A. = 0.70, air). A scrambled-laser source is used to increase intensity at high frequencies. We record the motions of particles at 30 and 3700 frames/sec using a fast digital camera (Phantom v5) with an exposure time of 260 μs, yielding a frequency range of nearly 5 decades from 0.05 to 2000 rad/sec. To reduce the noise of two-particle displacement correlation, we image about 100 particles in the field of view, capture several thousand frames, and average over eight sets of data. Particle centers are identified in each frame to an accuracy of 20 nm and particle trajectories are determined [17] to calculate the ensemble averaged mean-squared displacement $\langle \Delta x^2(\tau) \rangle$ (1P MSD).

For a solution of 1.0 mg/mL F-actin with $\xi = 0.3$ μm, the filament length qualitatively alters the time evolution of the 1P MSD. For $L = 0.5$ μm, the 1P MSD evolves as $\sim \tau^{0.85}$ over the entire frequency range probed, as shown by the open symbols in Fig. 1(a), indicating that the sample is close to a Newtonian fluid. By contrast, for longer filaments, the particle motion shows a transition between two regimes of temporal evolution. When $L = 2$ μm, the 1P MSD evolves as $\sim \tau^{0.75}$ below 0.01 sec and crosses over to show little time evolution after 0.1 sec, as shown by the open symbols in Fig. 1(b). Similar behavior is observed when L is increased to 5 μm and to 17 μm, as shown by the open symbols in Figs. 1(c) and 1(d) respectively. At long times (>0.1 sec), the 1P MSD depends on L for $L \geq 2$ μm and becomes more constrained as L is increased. Moreover, for different L, there is remarkable similarity in the short-time (<0.01 sec) behavior of the 1P MSD and in the crossover time τ_c between the two regimes.

To probe dynamics at lengths much larger than a, we use 2P microrheology. We calculate the 2P displacement correlation tensor, and scale this to a (2P MSD) [14,15]. Physically, the 2P MSD reflects extrapolation of long-wavelength thermal fluctuations of the medium to the particle size [14]. Because it measures the correlation of pairs of particles, 2P MSD is inherently noisier than 1P MSD. However, the qualitative features of 2P MSD are robust. When $L \approx a$, 2P MSD matches 1P MSD reasonably well over the entire frequency range, as shown by the closed symbols for $L = 0.5$ μm in Fig. 1(a). However, a discrepancy in both magnitude and time dependence is observed for $L > a$. For instance, for $L = 2$ μm, the 2P MSD is an order of magnitude smaller than the 1P MSD at $\tau = 0.1$ sec, as shown by the closed symbols in Fig. 1(b); moreover, it scales as $\tau^{0.7}$ whereas the 1P MSD shows little time evolution after 0.1 sec. Similar discrepancy is observed as L is increased to 5 μm and 17 μm, as shown by the closed symbols in Figs. 1(c) and 1(d) respectively. For all the samples with $L \geq 2$ μm, the 2P MSD is about an order of magnitude smaller than the 1P MSD at $\tau = 0.1$ sec, and exhibits a scaling τ^{α} with exponent α varying

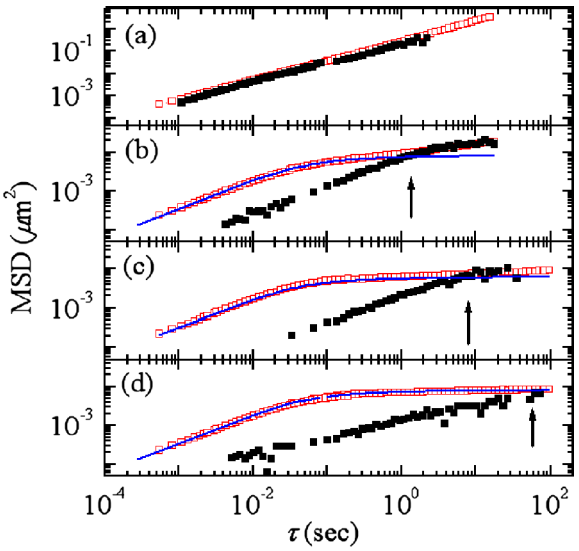

FIG. 1 (color online). Comparison of one-particle (open symbols) and two-particle (closed symbols) MSDs in 1.0 mg/mL F-actin with particle radius $a = 0.42$ μm for average filament length (a) 0.5 μm, (b) 2 μm, (c) 5 μm, and (d) 17 μm. The arrows in (b), (c), and (d) indicate the time when 1P and 2P MSDs converge. The solid lines through the data show the best fit to the 1P MSD using the model described in the text; the slight discrepancy at long times reflects effects of filament reptation, which are not included in the theory.

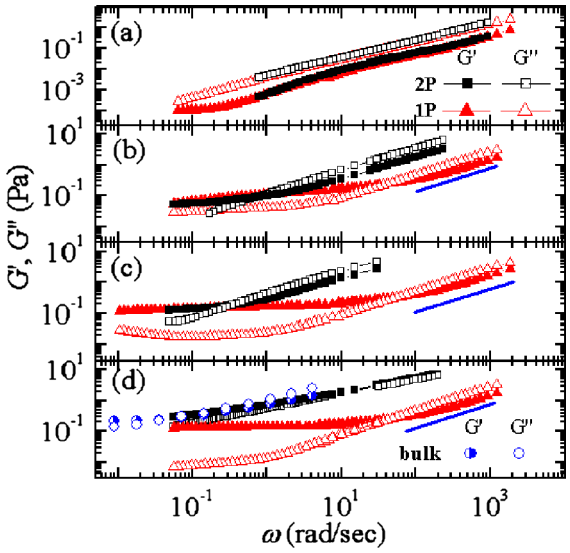

FIG. 2 (color online). Comparison between the elastic modulus, $G'(\omega)$ (closed symbols), and loss modulus, $G''(\omega)$ (open symbols) obtained from one-particle (triangles) and two-particle (squares) microrheology for average filament length (a) 0.5 μm, (b) 2 μm, (c) 5 μm, and (d) 17 μm. $G'(\omega)$ (half filled circles) and $G''(\omega)$ (circles) obtained from bulk rheology are shown in (d). The solid lines in (b), (c), and (d) show a scaling of $\omega^{3/4}$.

from 0.7 to 0.5. Compared to the insensitivity of the 1P MSD to filament length, the 2P MSD exhibits changes in both slope and magnitude as L is varied. Remarkably, despite their discrepancies, the 1P and 2P MSDs converge to similar values at a time scale, τ_m, as indicated by the arrows; τ_m increases dramatically as L is increased.

Using the generalized Stokes-Einstein relation, we interpret 1P and 2P MSDs to obtain a good approximation of the viscoelasticity probed by 1P and 2P microrheology, respectively [18]. When $L = 0.5$ μm, the 1P and 2P microrheology match reasonably well over the entire frequency range, as shown by the triangles and squares, respectively, in Fig. 2(a); G'' dominates and shows a scaling $\omega^{0.85}$ over the frequency range probed. However, as the filament length is increased, we observe a dramatic difference between the 1P and 2P microrheology, as shown by the triangles and squares, respectively, in Figs. 2(b)–2(d). Similar behavior is observed for the 1P microrheology for samples with $L \geq 2$ μm. For $\omega > 30$ rad/sec, G' and G'' scale as $\omega^{3/4}$, as indicated by the solid lines; whereas for $\omega < 30$ rad/sec, a plateau is observed for G'. The transition is rapid and occurs at approximately the same frequency for samples with $L \geq 2$ μm. In contrast to the insensitivity of 1P microrheology to L, 2P microrheology shows enhanced viscoelasticity that is L dependent. Moreover, it agrees well with the results of macroscopic rheology [4], shown by the circles in Fig. 2(d); this confirms the robustness of the 2P data. However, despite these discrepancies, the 1P and 2P elastic moduli converge to similar values at the lowest frequencies. The convergence to a plateau is not obvious for $L = 17$ μm due to poor statistics of the 2P data at low frequencies. However, the bulk data shows a clear plateau below $\sim$0.05 rad/sec. The convergence frequency of the 1P and 2P elastic moduli is proportional to τ_m^{-1}, decreasing dramatically as L increases.

To elucidate the origin of the discrepancy between 1P and 2P microrheology, we quantify the dependence of τ_c and τ_m on L. For a more accurate estimation of τ_c, we determine the retardation spectra from regularized fits to the 1P MSDs [19]. The value of τ_c obtained from the peak in the spectrum is independent of L, as shown by the open symbols in Fig. 3. By contrast, τ_m is strongly dependent on L, as shown by the closed symbols in Fig. 3, and scales as $\tau_m \sim L^2$, as shown by the dashed line.

The 1P microrheology probes the viscoelastic behavior at length scales of $2a \sim 0.84$ μm. Above $\tau_c^{-1} \sim$ 30 rad/sec, it is remarkably insensitive to L and shows a frequency dependence that is compatible with $\omega^{3/4}$. This suggests that 1P microrheology probes bending fluctuations of single filaments at these frequencies. In this regime, single-filament dynamics dominate the mechanical response until filaments become sterically hindered at the entanglement length. The characteristic time scale for bending fluctuations to relax over l_e is $\tau_e \approx \varsigma l_e^4/l_p k_B T$

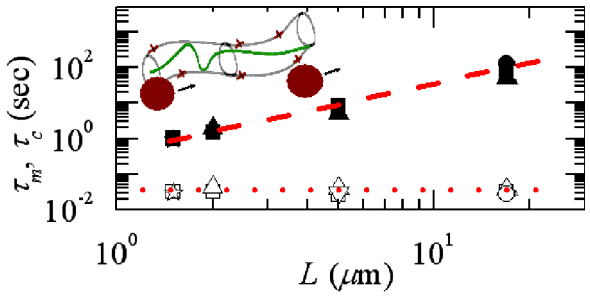

FIG. 3 (color online). The filament-length dependence of τ_m (closed symbols) and τ_c (open symbols) in 1.0 mg/mL F-actin with particle radius $a = 0.42$ μm. Different symbols represent data from different experiments. The dashed line shows a scaling of L^2. The dotted line shows a scaling of L^0. The inset is a schematic sketch showing longitudinal density fluctuations of a filament confined in a tube due to the presence of other filaments. Correlated motion of two separated particles couples to these fluctuations.

[12]. This time scale has no dependence on L, consistent with our observation for τ_c in Fig. 3. The independence was also seen at a higher concentration [13]. At frequencies below $\tau_c^{-1} \sim 30$ rad/sec, 1P microrheology shows an elastic plateau for samples with the longest filaments. The concentration dependence of the 1P plateau modulus G_0 for $L = 17$ μm, shown by the symbols in Fig. 4(a), is in good agreement with theoretical estimates [3,4], shown by the solid line. This elastic plateau results from steric hindrance of the filaments at the entanglement length. The modulus probed by the 1P mircorheology for $\omega < \tau_c^{-1}$ apparently corresponds to this plateau. For a small bead that couples to single-filament eigenmodes that are them-

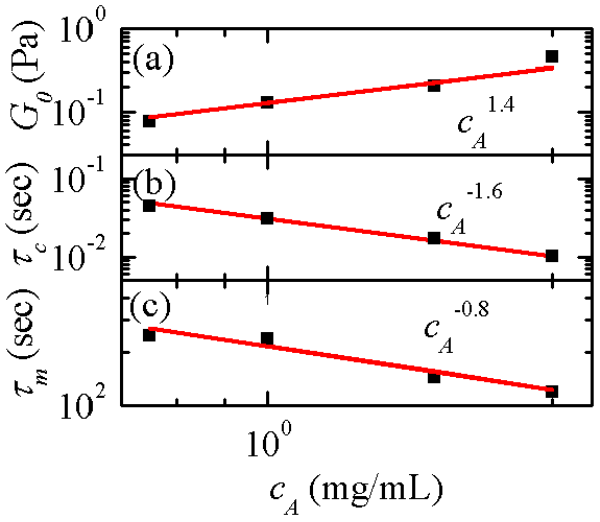

FIG. 4 (color online). The concentration dependence of (a) the plateau modulus, G_0 (symbols), (b) τ_c (symbols), and (c) τ_m (symbols). The lines in (a), (b), and (c) show the scaling indicated. The average filament length is 17 μm and the particle radius is 0.42 μm.

selves coupled to collective modes of an overdamped elastic background, the 1P MSD is $\Delta x^2(t) = A\{1 - (\pi/t)^a \mathrm{erf}(t^a)/2\} + B\{1 - bt^b\Gamma[-b, t]\}$, where $a = 1/2$, $b = 3/4$, Γ is the incomplete Gamma function, and t is in units of τ_c [20]. The best fits for this model are in good accord with experiment, as shown by the solid lines through the 1P MSD's in Fig. 1, except at the longest times, where filament reptation leads to further increases.

In contrast to 1P microrheology, 2P microrheology shows enhanced viscoelastic relaxation which is filament-length dependent at intermediate frequencies. The relaxation time of this extra dissipation can be identified as τ_m, which scales as $\tau_m \sim L^2$, as shown in Fig. 3. This is reminiscent of diffusion, consistent with longitudinal density fluctuations that relax diffusively up to l_p [3,12], as shown schematically in the inset of Fig. 3. Transverse thermal fluctuations in the filament lead to fluctuations in the quantity of material present in each segment of l_e; these density fluctuations diffuse along the filament [2]. Thus the lowest frequency of these excitations that affect 2P microrheology is determined by the time taken for the fluctuations to diffuse a filament length, $\tau_L \approx \tau_e(L/l_e)^2$ [12]. However, 1P microrheology fails to probe contributions from these long-wavelength fluctuations because 1P motion can sense only fluctuations on length scales of the bead size, which relax much faster [21]. By contrast, 2P microrheology does sense these fluctuations because it probes motion at much longer length scales. Therefore, 1P microrheology underestimates the bulk response, and the difference between 1P and 2P microrheology disappears when $\omega < \tau_L^{-1}$, as the long-wavelength longitudinal fluctuations have diffusively dissipated. The 2P microrheology shows that this additional relaxation leads to $G'(\omega) \sim G''(\omega) \sim \omega^{1/2}$; this scaling behavior is not predicted theoretically [3,12].

As a further test, we compare the concentration dependence of the time scales to theoretical predictions. The c_A dependence of τ_c, shown by the symbols in Fig. 4(b) is in excellent agreement with the theoretical prediction $\tau_e \sim l_e^4 \sim c_A^{-1.6}$, shown by the solid line. The c_A dependence of τ_m, shown by symbols in Fig. 4(c), is also in excellent agreement with the prediction $\tau_L \sim \tau_e/l_e^2 \sim c_A^{-0.8}$ [12], shown by the solid line.

All our results are obtained using 0.42 μm polystyrene particles; we find no a dependence and observe similar behavior for particles up to $a = 1$ μm. By comparison, measurements using silica particles and a two-laser tracking system did exhibit an a dependence for $a = 2.5$ μm [22]. A deviation between the 1P and 2P microrheology was attributed to effects of depletion [3]. While we see no convincing evidence of this, it is conceivable that there are slight effects of adhesion for either set of particles, leading to the difference. Measurements using magnetic beads with $a = 2.25$ μm reported a lower crossover frequency than our results [13]. We hypothesize that these particles probe lengths intermediate between those probed with 1P and 2P microrheology. However, our essential conclusion is robust and independent of small measurement discrepancies.

These results suggest that in entangled F-actin solutions, the mechanical response changes as the different length scales in the system vary. Microrheology can be used to probe length-scale-dependent rheology. Moreover, the results also suggest that 1P microrheology may be more useful for measurements of cross-linked networks of semiflexible filaments, where contributions from long-wavelength longitudinal fluctuations are reduced. The results highlight the sensitivity of the rheology of entangled solutions of semiflexible polymers to the length scales that determine both network geometry and filament properties; this provides new insight into the origin of the scaling behavior of the rheology that has yet to be fully described theoretically.

We thank T. Stossel for the gelsolin, A. Popp and B. Hinner for bulk rheology data, F. MacKintosh and G. Koenderink for valuable discussions, and K. Miranda and G. Massiera for assistance. This work was supported by the NSF (DMR-0243715), the Harvard MRSEC (DMR-0213805), and in part by Lucent GRPW (M. L. G.).

*Present address: Department of Cell Biology, The Scripps Research Institute, La Jolla, CA 92037, USA.

[1] F. Gittes and F. C. MacKintosh, Phys. Rev. E **58**, R1241 (1998).
[2] A. C. Maggs, Phys. Rev. E **55**, 7396 (1997).
[3] D. C. Morse, Macromolecules **31**, 7044 (1998).
[4] B. Hinner *et al.*, Phys. Rev. Lett. **81**, 2614 (1998).
[5] F. Amblard *et al.*, Phys. Rev. Lett. **77**, 4470 (1996).
[6] A. Semenov, J. Chem. Soc., Faraday Trans. 2 **82**, 317 (1986).
[7] A. Ott *et al.*, Phys. Rev. E **48**, R1642 (1993).
[8] F. Gittes *et al.*, J. Cell Biol. **120**, 923 (1993).
[9] E. H. Egelman, J. Muscle Res. Cell Motil. **6**, 129 (1985).
[10] C. F. Schmidt *et al.*, Macromolecules **22**, 3638 (1989).
[11] P. A. Janmey *et al.*, J. Biol. Chem. **261**, 8357 (1986).
[12] H. Isambert and A. C. Maggs, Macromolecules **29**, 1036 (1996).
[13] F. G. Schmidt *et al.*, Phys. Rev. E **61**, 5646 (2000).
[14] J. C. Crocker *et al.*, Phys. Rev. Lett. **85**, 888 (2000).
[15] M. L. Gardel *et al.*, Phys. Rev. Lett. **91**, 158302 (2003).
[16] M. T. Valentine *et al.*, Biophys. J. **86**, 4004 (2004).
[17] J. C. Crocker and D. G. Grier, J. Colloid Interface Sci. **179**, 298 (1996).
[18] T. G. Mason, Rheol. Acta **39**, 371 (2000).
[19] T. G. Mason *et al.*, J. Rheol. (N.Y.) **44**, 917 (2000).
[20] K. Kroy and E. Frey, in *Scattering in Polymeric and Colloidal Systems*, edited by W. Brown and K. Mortensen (Gordon and Breach, New York, 2000).
[21] A. C. Maggs, Phys. Rev. E **57**, 2091 (1998).
[22] M. Atakhorrami *et al.* (to be published).